Lawrence Berkeley National Laboratory
Recent Work

Title
CALCULATIONS WITH THE NUCLEAR FIRESTREAK MODEL

Permalink
https://escholarship.org/uc/item/4dp37221

Author
Gosset, J.

Publication Date
1978-03-01

eScholarship.org Powered by the California Digital Library
University of California

Submitted to Physical Review C

LBL-7139
Preprint

CALCULATIONS WITH THE NUCLEAR FIRESTREAK MODEL

J. Gosset, J. I. Kapusta, and
G. D. Westfall

March 1978

Prepared for the U. S. Department of Energy
under Contract W-7405-ENG-48

TWO-WEEK LOAN COPY

This is a Library Circulating Copy
which may be borrowed for two weeks.
For a personal retention copy, call
Tech. Info. Division, Ext. ~~5716~~ 6782

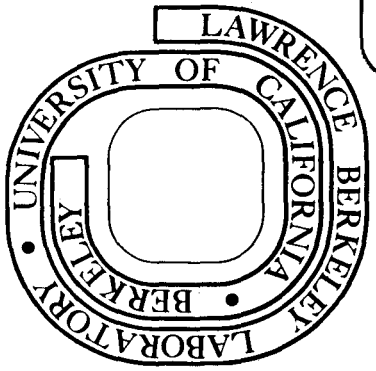

LBL-7139 c.2

DISCLAIMER

This document was prepared as an account of work sponsored by the United States Government. While this document is believed to contain correct information, neither the United States Government nor any agency thereof, nor the Regents of the University of California, nor any of their employees, makes any warranty, express or implied, or assumes any legal responsibility for the accuracy, completeness, or usefulness of any information, apparatus, product, or process disclosed, or represents that its use would not infringe privately owned rights. Reference herein to any specific commercial product, process, or service by its trade name, trademark, manufacturer, or otherwise, does not necessarily constitute or imply its endorsement, recommendation, or favoring by the United States Government or any agency thereof, or the Regents of the University of California. The views and opinions of authors expressed herein do not necessarily state or reflect those of the United States Government or any agency thereof or the Regents of the University of California.

CALCULATIONS WITH THE NUCLEAR FIRESTREAK MODEL

J. Gosset

J. I. Kapusta

G. D. Westfall

LBL Report No. 7139

Submitted to Physical Review C.

March, 1978

CALCULATIONS WITH THE NUCLEAR FIRESTREAK MODEL*

J. Gosset†, J. I. Kapusta and G. D. Westfall

Lawrence Berkeley Laboratory, Berkeley, CA 94720

ABSTRACT

A model is presented which is capable of calculating simultaneously the spectra of pions, nucleons and light nuclei from the collision of relativistic heavy ions. It is based on the nuclear fireball model, the geometrical picture of Myers, and the nuclear thermodynamics of Mekjian and Kapusta. Maximum use is made of the conservation laws for baryon number, charge, energy, momentum and angular momentum. Single particle inclusive cross sections were calculated and compared with experiment for a wide range of beam energies and observed fragments. Except for some conflicting normalizations and high energy pions good agreement is found. The density at which hadrons effectively cease to interact, which is the only parameter in the model, is determined to be 0.12 hadrons/fm^3.

---

*This work was supported by Nuclear Physics Division of the U.S. Department of Energy.

†Permanent address: DPhN/ME, Centre d'Etudes Nucléaires de Saclay, 91190 Gif-sur-Yvette, France.

Key Words

NUCLEAR REACTIONS

Relativistic heavy ions; firestreaks, hadronic thermal equilibrium; calculated differential cross sections of $\pi^{\pm}$, p, d, t, ^{3}He, ^{4}He; comparisons with experiment.

I. INTRODUCTION

Recently a large amount of experimental data concerning relativistic heavy ion reactions has become available.[1-4] The data considered here consist of single particle inclusive spectra of pions, nucleons, and light nuclei up to ^{4}He. These spectra were measured for a variety of target-projectile-incident energy combinations over a wide range of observed energies and angles. Several models[5] have been proposed to predict the nucleon spectra produced in these collisions including the nuclear fireball model,[6] the firestreak model,[7] intranuclear cascade,[8-10] hydrodynamics,[9-11] row on row,[12] and nucleon knock-out.[13] The light nuclei spectra have been interpreted in terms of the coalescence model,[14] equilibrium thermodynamics,[15] and the sudden approximation in quantum mechanics.[16] An explanation of the low energy pion spectra has been attempted in terms of the superposition of proton-nucleus results. Pion production has also been interpreted within the framework of the fireball model.[17]

It is hoped that in relativistic heavy ion collisions, new phenomena can be studied such as density isomers or pion condensates.[18] However, the calculation of observable quantities resulting from these exotic phenomena are not yet possible. A calculation incorporating known phenomena would be useful in predicting what one would expect to observe in these reactions if nothing unusual were taking place. Such a model must be simple enough to allow comparison with data and yet must include enough realistic features to make a comparison reasonable. These features should include a description of the size and shape of nuclei, incorporation of conservation laws, and the concept that many "interactions" take place during the collision.

Presented here is a macroscopic model capable of simultaneously predicting the pion, nucleon, and light nucleus inclusive spectra resulting from relativistic heavy ion collisions. The model is based on the geometrical and kinematical assumptions used in the firestreak model[7] including diffuse nuclear density distributions. Also included is equilibrium thermodynamics[15,17] solved self-consistently to obtain the relative concentrations and distribution function of the various particles produced in these collisions. This model will be referred to as "The Nuclear Firestreak Model."

In Section II a detailed description of the model is presented followed by a comparison to the existing data in Section III.

II. DESCRIPTION OF THE MODEL

The basic philosophy is similar to the one in the nuclear fireball model[6] which was used to calculate the proton inclusive spectra from relativistic heavy ion collisions. One assumed that there were enough "interactions" for thermodynamic equilibrium to occur between the nucleons that participate in the reaction. These nucleons form a fireball which decays as an ideal gas. This simple model is deficient in two significant respects. First it is necessary to explain not only the production of nucleons in these collisions but also the copious production of the composite fragments as well as of pions. The thermodynamic equilibrium between nucleons has been generalized to a chemical equilibrium between the various hadronic species through the use of a chemical potential.[15,17] The one variable parameter which has been introduced in the model is the critical density at which equilibrium is reached

and below which the momentum distribution of the fragments does not vary because they are no longer interacting. This critical density has also been called the freeze-out or break-up[16] density. The second deficiency is the drastic geometrical assumptions used in the nuclear fireball model of sharp spheres and clean cylindrical cuts between the colliding nuclei. The treatment of nuclear density distributions with diffuse surfaces[7] leads to a temperature gradient across the fireball according to the relative amounts of material coming from the target and the projectile.

Thus the model describes relativistic heavy ion collisions by assuming that the interaction between the nuclei is localized to the overlapping volume. In this volume the interaction proceeds via colinear streaks of nuclear matter from the target and projectile that undergo completely inelastic collisions. This nuclear matter is treated as a thermodynamic system in chemical equilibrium which allows the calculation of the relative concentrations of pions, nucleons and light nuclei and their distribution functions. The firestreak geometry explicitly conserves angular momentum whereas it is well known that the fireball geometry does not. At low energy ($\lesssim$ 1 GeV/nucleon) this angular momentum nonconservation is not an important effect, whereas at high energy it is. Of course in this model one cannot investigate the detailed time development of the collision since there are no equations of motion.

In this section we present the model in detail with respect to the geometry and kinematics first, and then to the thermodynamics.

1. Geometry and Kinematics

To treat nuclear density distributions with diffuse surfaces one can subdivide the projectile and target into infinitesimal streaks

parallel to the relative motion of the colliding nuclei.[7] Each of these streaks is characterized completely by the relative amount η of material coming from the projectile. Here $\eta = N_p/(N_p + N_T)$ where N_p and N_T are the number of contributing nucleons from the projectile and target. It should be noted that η is in principle a continuous variable, but for computational purposes is taken to be discrete. The velocity β of the streak center of mass and its rest mass M depend only on this parameter η. The expression for calculating any observable involves in principle a double summation over this parameter η and over the impact parameter. Since η defines completely the collision for any single particle observable, this double summation can be partially done over the impact parameter.[19] The Lorentz invariant momentum space densities F_j for particles of type j which are produced in the collision can be expressed as a sum of terms, each of which is factorized into a geometrical part, which is the yield function $Y(\eta)$, and the Lorentz invariant momentum space density f_j for particles of type j emitted by a system of mass $M(\eta)$ moving in the laboratory at the velocity $\beta(\eta)$:

$$F_j(\vec{p}) = \sum_{i=1}^{N} Y(\eta_i)\, f_j\, [\vec{p};\, M(\eta_i),\, \beta(\eta_i)]. \qquad (1)$$

The yield function Y, in units of cross section, contains all the geometrical aspects of the problem.

One defines $w_b(x,y)$ as the combined target-projectile density distribution projected onto the x-y plane perpendicular to the beam. The yield function is calculated by integrating $w_b(x,y)$ over impact parameter b and over the x-y plane:

$$Y(\eta_i) = \int_{\eta_i - \frac{1}{2}\delta\eta}^{\eta_i + \frac{1}{2}\delta\eta} d\eta' \int 2\pi b db \iint dx dy \; w_b(x,y) \; \delta[\eta' - \eta_b(x,y)]. \quad (2)$$

Throughout this paper the yield functions tabulated in Ref. 7 will be used.

Each term of the summation (1) corresponds to a streak having a charge to baryon number ratio Q/B of

$$\frac{Q}{B} = \eta \frac{Z_p}{A_p} + (1-\eta) \frac{Z_t}{A_t} \quad , \quad (3)$$

where Z_i and A_i are respectively the charge and baryon numbers of the projectile (i = p) and target (i = t) nuclei. The laboratory velocity of the streak center of mass is:

$$\beta = \frac{P_{lab}}{E_{lab}} \quad . \quad (4)$$

P_{lab} and E_{lab} are the laboratory momentum and total energy of the streak. This velocity can be rewritten in terms of η as:

$$\beta = \frac{\eta[t(t + 2m')]^{1/2}}{m' + \eta t} \quad (5)$$

Here t is the laboratory kinetic energy per nucleon of the projectile and m' is the bound nucleon mass. The rest mass of the streak is:

$$M = (E_{lab}^2 - P_{lab}^2)^{1/2} \quad , \quad (6)$$

which can also be rewritten in terms of η as:

$$\frac{M}{B} = m' \left[1 + 2\eta(1-\eta) \frac{t}{m'}\right]^{1/2} \quad . \quad (7)$$

Taking into account the neutron-proton mass difference, which has been done in the calculations presented in this paper, leads to slightly more complicated formulae than eqs. (5) and (7) for β and M.

2. Thermodynamics

The Lorentz invariant momentum space densities f_j can be calculated in any reference frame, in particular in the streak center of mass frame where $\vec{p}$ is Lorentz transformed into $\vec{p}'$ and β is equal to zero:

$$f_j\,[\vec{p};\, M(\eta_i), \beta(\eta_i)] = f_j\,[\vec{p}';\, M(\eta_i),\, 0] \quad . \tag{8}$$

These momentum space densities follow from the assumption of thermodynamic equilibrium between all possible nuclear species at the given critical hadron density ρ_c. They are isotropic in the streak center of mass frame with a Fermi or Bose distribution:

$$f_j(\vec{p}') = E' \frac{d^3N_j}{dp'^3} = E' \frac{(2S_j + 1)V}{(2\pi)^3} \left[\exp \frac{E' - \mu_j}{T} \pm 1\right]^{-1} \tag{9a}$$

$$\rightarrow E' \frac{(2S_j + 1)V}{(2\pi)^3} \exp\left(\frac{\mu_j - m_j}{T}\right) \exp\left(\frac{-p'^2}{2m_j T}\right) \quad . \tag{9b}$$

The arrow indicates the classical statistics nonrelativistic limit. The quantity m_j is the mass of the particle, E' its total energy equal to $(p'^2 + m_j^2)^{1/2}$, S_j and μ_j its spin and chemical potential. V and T are respectively the volume and the temperature of the system at the critical density. The + or - sign refers to fermion or bosons. We use $\hbar = c = k = 1$.

The statement of thermal equilibrium implies certain relations among the chemical potentials. For example $n + n + p \leftrightarrow n + d$ implies that $\mu_d = \mu_n + \mu_p$ and $p + n \leftrightarrow n + n + \pi^+$ implies that $\mu_{\pi^+} = \mu_p - \mu_n$. The chemical potentials of all the hadrons are linear combinations of the neutron and proton chemical potentials μ_n and μ_p. Since we want to calculate composite particle production up to ^{4}He, as well as pion production, it is necessary to include in the chemical equilibrium at least pions, neutrons, protons, deuterons, tritons, ^{3}He and ^{4}He. It is well known that at the energies considered in this paper, pion production proceeds mainly through the formation and decay of the Δ resonance. This baryonic resonance is taken into account in the chemical equilibrium with its four charge states. In contrast to Ref. 17 the wide mass spectrium of the Δ is approximated by nine discrete masses at regular intervals from threshold and symmetrically arranged around the central value of 1232 MeV. Each mass is given a weight from a single-level resonance formula[20] and the total weight is normalized to 1. Since a species with such a short lifetime is introduced in the system we should also take into account the effect of the excited unbound states of composite fragments, as already suggested in Ref. 15, up to mass 5 for calculating ^{4}He production. Because of their great number[21-23] they are grouped together as shown in Table 1 with an effective excitation energy, degeneracy $(2S + 1)$ and decay mode(s) for each one of the nuclear species ^{2}H, ^{4}He, ^{4}He, ^{4}Li, ^{5}He and ^{5}Li. These resonances, baryonic as well as nuclear, are supposed to leave the equilibrium

region intact and naturally decay afterwards by particle emission into pions, nucleons and stable-light nuclei. The stable particle spectra thus consist of a sum of two components, a thermal one given by Eq. (9) and a resonance two-body decay one, resulting from all the possible two-body decays of resonances which are themselves emitted with a thermal spectrum given by Eq. (9). As shown in Ref. 17, this second component can be written:

$$f_j(\vec{p}') = \sum_R \frac{W_D (2S_R+1) V m_R T^2}{16\pi^3 p' p_D} \left[\frac{\mu_R}{T} \log(1+e^{-x}) + \sum_{n=1}^{\infty} \frac{(\mp)^{n+1}}{n^2} e^{-nx}(nx+1) \right]_{x_+}^{x_-} \qquad (10)$$

$$\text{where } Tx_{\pm} = \frac{m_R}{m_j^2} (E'E_D \pm p'p_D) - \mu_R \quad . \qquad (11)$$

Here S_R, m_R and μ_R are the spin, mass and chemical potential of the resonance R. W_D is the branching ratio for the decay of the resonance R into the particle of type j. The quantities p_D and E_D are the decay momentum and total energy of the particle of type j in the rest frame of the resonance R.

The thermodynamical problem can thus be summarized in the following way. For each value of the projectile relative anount η we have to find the neutron and proton chemical potentials μ_n and

μ_p, the temperature T and the volume V of a system in thermodynamical equilibrium with baryon number B, charge Q, and total mass M at hadron density ρ_c. The total number N_j and average energy E_j (including rest mass) of each type j of particle or resonance can be obtained by integrating Eq. (9) with the proper integrand:

$$N_j = \frac{(2S_j + 1)Vm_j^2 T}{2\pi^2} \sum_{n=1}^{\infty} \frac{(\mp)^{n+1}}{n} \exp\left(\frac{n\mu_j}{T}\right) K_2\left(\frac{nm_j}{T}\right) \tag{12a}$$

$$\rightarrow (2S_j+1)V\left(\frac{m_j T}{2\pi}\right)^{3/2} \exp\left(\frac{\mu_j - m_j}{T}\right) , \tag{12b}$$

and

$$N_j E_j = \frac{(2S_j+1)Vm_j^3 T}{2\pi^2} \sum_{n=1}^{\infty} \frac{(\mp)^{n+1}}{n} \exp\left(\frac{n\mu_j}{T}\right)\left[K_1\left(\frac{nm_j}{T}\right) + \frac{3T}{nm_j} K_2\left(\frac{nm_j}{T}\right)\right] \tag{13a}$$

$$\rightarrow N_j\left(m_j + \frac{3}{2} T\right) . \tag{13b}$$

The volume dependence is very simple. The number and energy densities depend only on the three variables μ_n, μ_p and T. For any set of values of these variables, it is possible to calculate the baryon (b), charge (q), energy (e) and hadron (h) densities:

$$b(\mu_n,\mu_p,T) = \sum_j \left(\frac{N_j}{V}\right) B_j \quad , \tag{14}$$

$$q(\mu_n,\mu_p,T) = \sum_j \left(\frac{N_j}{V}\right) Q_j \quad , \tag{15}$$

$$e(\mu_n, \mu_p, T) = \sum_j \left(\frac{N_j}{V}\right) E_j \quad , \tag{16}$$

and $$h(\mu_n, \mu_p, T) = \sum_j \left(\frac{N_j}{V}\right) H_j \quad , \tag{17}$$

where B_j, Q_j and H_j are the baryon, charge and hadron quantum numbers of particles or resonances of type j. There remain only three equations to be solved for μ_n, μ_p and T, for example :

$$\begin{aligned} e/b &= M/B \\ q/b &= Q/B \\ h &= \rho_c \end{aligned} \tag{18}$$

and the volume V will follow from the solution to these equations, being simply equal to B/b. The system of equations (18) is not linear in μ_n, μ_p and T. It is solved by a least square method, minimizing the function :

$$\chi^2(\mu_n,\mu_p,T) = \left(\frac{e/b}{M/B} - 1\right)^2 + \left(\frac{q/b}{Q/B} - 1\right)^2 + \left(\frac{h}{\rho_c} - 1\right)^2 \quad , \tag{19}$$

with the starting guess being the classical statistics, nonrelativistic case with only nucleons.[24]

III. COMPARISON WITH EXPERIMENT

In this section, the predictions of the nuclear firestreak model will be compared with most of the available data on single particle inclusive differential cross sections. These comparisons cover beam energies from 400 to 2100 MeV per nucleon (MeV/nucleon). The observed fragments range from π to ^{4}He depending on the experiment. All of the calculations presented here were performed with the same value of the critical density ρ_c which will be discussed below. All of the calculations were performed including both the ground and excited states of the light nuclei and including pions as discussed in section II. The effect of neglecting the excited states will be discussed below. Finally the range of the variable η appearing in the yield function $Y(\eta)$ was taken to be beam energy dependent. The value of η_{min} (with $\eta_{max} = 1 - \eta_{min}$) was chosen so that the resultant excitation energy per baryon was 5 to 10 MeV above the continuum. The part of $Y(\eta)$ which is not included contributes predominantly to the yield of higher mass nuclear fragments and thus is outside the scope of this paper. Although one may question the wisdom of discussing such fine points in a model as simple as this one, nonetheless it is fruitful to examine the consequences of a consistent application of any model to pinpoint precisely those regions where the model fails.

First consider the bombardment of ^{238}U by a 400 MeV/nucleon ^{20}Ne beam.[1] The double differential cross section at fixed laboratory angle as a function of laboratory kinetic energy per nucleon for p,d,t, ^{3}He, and ^{4}He is shown in Figures 1 through 5 respectively. All of the theoretical curves have been multiplied by a factor of 2, except for

the special case of ^{4}He which will be discussed separately below.

The agreement of the calculated curves with the shape of data is excellent in all cases except for the 30° spectra. The shapes of the cross sections are essentially independent of the value of ρ_c. The magnitudes of the cross sections are somewhat dependent on ρ_c, the heavier the nuclear fragment the stronger the dependence. As ρ_c is increased over a reasonable range of values, the d yield decreases while the ^{4}He yield increases. A unique value of $\rho_c = 0.12 \pm 0.02$ hadrons/fm^3 was found for which the normalization discrepancy between theory and experiment was the same for p,d,t, and ^{3}He. Certainly there is no a priori reason to believe that such a value should exist. Indeed our attempt to fit the data by including only the bound light nuclei does not result in a unique value of ρ_c. It is significant that this density is slightly less than normal nuclear density because this allows the interpretation that some of the nucleons condense into composite states in a statistical manner when the density is low enough. These observations lend credence to the whole concept of light nuclei, both ground state and excited, being in thermal equilibrium at some critical density. In fact the fit is so good, considering that there is only one adjustable parameter,[25] that one should seriously entertain the possibility that the absolute normalization of the experiment is too high by a factor of 2. The estimated uncertainty in the absolute normalization was 30%. This would be a 1.7 standard deviation departure. If subsequent measurements confirm this normalization discrepancy then one must conclude that the model is missing some essential physics.

The theoretical curve for ^{4}He shown in Figure 5 was multiplied by a factor of 4. This additional factor of 2 may arise from several effects. Firstly a cut off has been placed at A = 5. The A = 4 nucleus is most sensitive to this cut off with the A = 1,2,3 nuclei being less sensitive. In addition ^{4}He is an exceptionally stable nucleus. Therefore many unstable higher mass states decay into ^{4}He but less so into d,t, or ^{3}He. Thus, depending on what aspects of the reaction one wishes to study, ^{4}He is or is not a good tool for investigation.

It should be noted in passing that the same calculations performed with the fireball geometry instead of the firestreak geometry with diffuse nuclear surfaces cannot reproduce the data on d,t,^{3}He and ^{4}He even in overall shape. This is true for all the data examined in this paper. This illustrates the importance of the diffuse nuclear surface in the model.

^{238}U was also bombarded by ^{20}Ne at 2100 MeV/nucleon.[1] There were experimental difficulties with the detection of p,d, and t but not of ^{3}He and ^{4}He. The shape of the cross section at a given angle was measured reliably but the normalization changed from run to run by factors of 2 or so. The 2100 MeV/nucleon data on p,d, and t shown in Figures 1 to 3 was renormalized angle by angle from the original presentation of portions of it.[26] To be consistent with the 400 MeV/nucleon comparison the theoretical curves have been uniformly multiplied by a factor of 2, except for ^{4}He which has been multiplied by a factor of 6. Thus we do not claim detailed agreement between theory and experiment. All we claim is that the shapes of the cross sections at given angle agree and that normalizations are well within an order of magnitude.

However, the angular distribution predicted by the model for ^{3}He and ^{4}He disagrees with the observed angular distribution which should be experimentally reliable. The theory seems to reproduce the difference between the 30° and 120° spectra but underestimates the 60° and 90° spectra.

The fragments p,d, and t from the bombardment of ^{9}Be and ^{63}Cu by an 1800 MeV/nucleon ^{40}Ar beam were measured in a recent experiment.[2] The Lorentz invariant cross section at given laboratory angle as a function of laboratory momentum is shown in Figures 6 to 8. The data and theory are shown with their absolute normalizations unchanged. The experimental absolute normalization uncertainties are estimated as 25% for Be and 10% for Cu. The critical density is ρ_c = 0.12 hadrons/fm^3 although the results don't change much if ρ_c is varied from 0.10 to 0.14. The model seems to represent the data fairly well at 14.7° although the tritons from Cu may be a little underestimated. At 5° however the model generally overestimates the data especially in the more central region corresponding roughly to 2 GeV/c for protons, 3 GeV/c for deuterons, and 4 GeV/c for tritons. This could be caused by a variety of mechanisms but the most obvious one should be mentioned. It could be that the assumption of completely inelastic collisions between tubes is breaking down and that the surfaces of the colliding nuclei are somewhat transparent. This would tend to decrease the cross sections at the most forward angles where the main contribution comes from less central collisions.

Finally we compare with the high energy protons and pions[3] and the low energy pions[4] from the bombardment of NaF and ^{208}Pb by ^{20}Ne at a beam energy of 800 MeV/nucleon. The uncertainty in absolute

normalization is estimated at around 25% for both sets of data. The higher energy data is plotted in Figures 9 to 12 in the form of the Lorentz invariant differential cross section as a function of rapidity at fixed transverse momentum. This is a Lorentz invariant way of presenting data over a large kinematic region. A Lorentz transformation along the beam axis just shifts all rapidities by a constant amount. Figures 13 and 14 show the low energy pions in the more conventional plot of double differential cross section as a function of energy at fixed laboratory angle. Figures 9 to 12 show the absolute normalization of both theory and experiment whereas the theoretical curves in Figures 13 and 14 have been mutliplied by 1/2. The model gives a good representation of the protons from Pb, but generally overestimates them from the much smaller target NaF although the shapes agree quite well.

The model overestimates the cross section for pion production as is evident from both the low and high energy data. Looking at the low energy pions note that the model does not give enough curvature in the spectrum. A larger curvature is indicative of forward-backward peaking which is more characteristic of elementary nucleon-nucleon collisions. Further analysis[4] shows that the shape of the spectrum is not consistent with the free space reaction $NN \rightarrow NN\pi$ either. Thus the pions are probably rescattering to some extent but not enough to reach thermal equilibrium. Consideration of the high energy pions leads to the same conclusion. More experiments need to be done with larger mass projectiles on Pb or U at various beam energies to get as far away as possible from the elementary $NN \rightarrow NN\pi$ reaction.

Finally, we can examine three quantities which in some sense summarize the calculations. Figure 15 shows the temperature as a

function of η for the beam energies 400,800, and 2100 MeV/nucleon. (The 1800 MeV/nucleon calculation is not shown.) Near the target ($\eta \approx 0$) and projectile ($\eta \approx 1$) the temperature is lowest because the available center of mass energy is less in those regions. Inclusion of pions and deltas lowers the temperature, especially at the higher beam energies since energy is required to create these particles. Inclusion of the light nuclei raises the temperature somewhat. This is because the binding of nucleons into nuclei converts mass energy to random motion, and the number of degrees of freedom in the system becomes smaller so that the energy per degree of freedom is higher. Note that the temperatures shown do not correspond precisely to effective temperatures measured in the laboratory because when the particles go out of thermal equilibrium the resonances decay and so add some net kinetic energy to the final state. Figure 16 shows the ratio of the number of nucleons to the to the baryon number in the final state, i.e. after all resonances have decayed. This ratio is smallest near the target and projectile where the temperatures are low. The formation of light nuclei is favored when the temperature is low. This graph nicely illustrates how much error is involved in neglecting the production of light nuclei. At 400 MeV/nucleon at <u>least</u> 35% of the baryon number is bound up in light nuclear fragments! Figure 17 shows the ratio of the number of pions to the baryon number in the final state. This ratio increases with beam energy. Also it is peaked in the central region where the available center of mass energy, and hence the temperature, is the highest.

IV. CONCLUSION

The Nuclear Firestreak Model predicts, with a large degree of success, the pion, nucleon, and light nucleus inclusive spectra from a large variety of projectile-target-incident energy combinations over a wide kinematic range. The simultaneous prediction of the pion, nucleon, and light nucleus spectra is in contrast to models such as hydrodynamics where only the nucleon spectra can be predicted, intranuclear cascade which can only predict pions and nucleons, or the coalescence model which predicts the light nuclei spectra based on the measured proton spectra.

The model incorporates one variable parameter, the freeze-out density, ρ_c, which is uniquely determined to be $0.12 \pm .02$ hadrons/fm^3. The model, however, says nothing about densities greater than ρ_c except that it assumes that the expansion from the initial compressed state to the break-up density is isoergic.

The diffuse nuclear density distributions incorporated in this model are necessary to reproduce the shape of the measured spectra, especially for the light nuclei. However, the pion spectra is insensitive to whether or not one uses diffuse nuclear surfaces. Light nuclei are produced primarily in those regions which have a dominant amount of matter coming from either the target ($\eta \approx 0$) or projectile ($\eta \approx 1$), whereas the pions are primarily produced in those regions in which the target and projectile contribute equal amounts ($\eta \approx 1/2$).

Consideration has been given to the breakdown of some of the assumptions in the model. The assumption of straight line trajectories could

break down, producing conical rather than cylindrical cuts through the nuclei. This effect would involve transverse spreading of the interaction region. The assumption of full momentum transfer between the tubes must break down in large impact parameter collisions where the two nuclei interact only through the diffuse tails of their density distributions. The inclusion of transparency or the treatment of these types of tubes in terms of nucleon-nucleon scattering could be incorporated. The model also does not consider pre-equilibrium emission. This effect would most strongly affect the pion spectra.

One can predict multiparticle correlations using this model as well as multiplicity distributions.[27] However, to obtain these results, it seems to be necessary to return to the full two dimensional integral over impact parameter and η.

The exact quantum field theory treatment of relativistic heavy ion reactions is probably not a realistic goal. However, the relatively good success of the Nuclear Firestreak Model may help point the way toward more comprehensive models or theories of these reactions.

ACKNOWLEDGMENTS

We are grateful to numerous members of the Nuclear Science Division of LBL for their critical comments and thought provoking questions regarding this work. In particular we thank W. D. Myers for allowing us the use of his computer code. We thank the authors of the experimental work (Refs. 1-4) for their cooperation and for allowing us to publish their results. For their carefully considered reading of the manuscript we thank W. D. Myers and A. M. Poskanzer.

REFERENCES AND FOOTNOTES

1. J. Gosset, H. H. Gutbrod, W. G. Meyer, A. M. Poskanzer, A. Sandoval, R. Stock, and G. D. Westfall, Phys. Rev. C 16, 629 (1977).

2. V. Perez-Mendez, A. L. Sagle, E. T. B. Whipple, F. Zarbakhsh, G. Igo, M. M. Gazzaly, J. B. Carroll, J. V. Geaga, J. B. McClelland, M. A. Nasser, H. Spinka, and R. Talaga, Lawrence Berkeley Laboratory Report, LBL-7278.

3. S. Nagamiya, I. Tanihata, S. Schnetzer, L. Anderson, W. Brückner, O. Chamberlain, G. Shapiro, and H. Steiner, Lawrence Berkeley Laboratory Report, LBL-6770.

4. K. Nakai, J. Chiba, I. Tanihata, S. Nagamiya, H. Bowman, J. Ioannou, and J. O. Rasmussen, Proceedings of the International Conference on Nuclear Structure, Tokyo, Japan, Vol. 3, September, 1977; and private communication.

5. For a comparison of the different models see M. Gyulassy, Lawrence Berkeley Laboratory Report, LBL-6594, and proceedings of International Symposium on Nuclear Collisions and their Microscopic Description, Bled, Yugoslavia, September 25-October 1, 1977.

6. G. D. Westfall, J. Gosset, P. J. Johansen, A. M. Poskanzer, W. G. Meyer, H. H. Gutbrod, A. Sandoval, and R. Stock, Phys. Rev. Lett. 37, 1202 (1976), and Ref. 1.

7. W. D. Myers, Lawrence Berkeley Laboratory Report, LBL-6569 and Nucl. Phys., to be published. Myers coined the word firestreak to refer to this model when thermal distributions are used.

8. R. K. Smith and M. Danos, Proceedings of Meeting on Heavy Ion Collisions, Fall Creek Falls, Tennessee, June, 1977, and to be published.

9. A. A. Amsden, J. N. Ginocchio, F. H. Harlow, J. R. Nix, M. Danos, E. C. Halbert, R. K. Smith, Phys. Rev. Lett. 38, 1055 (1977).

10. J. P. Bondorf, H. T. Feldmeier, S. Garpman, and E. C. Halbert, Phys. Lett. 65 B, 217 (1976) and Z. Phys. 279, 385 (1976).

11. A. A. Amsden, F. H. Harlow, J. R. Nix, Los Alamos Laboratory Report LA-UR-77-31 (January 1977).

12. J. Hufner and J. Knoll, Nucl. Phys. A290, 460 (1977).

13. S. E. Koonin, Phys. Rev. Lett. 39, 680 (1977).

14. H. H. Gutbrod, A. Sandoval, P. J. Johansen, A. M. Poskanzer, J. Gosset, W. G. Meyer, G. D. Westfall, and R. Stock, Phys. Rev. Lett. 37, 667 (1976) and Ref. 1.

15. A. J. Mekjian, Phys. Rev. Lett. 38, 640 (1977) and "Explosive Nucleosynthesis, Equilibrium Thermodynamics and Relativistic Heavy Ion Collisions", Lawrence Berkeley Laboratory Report, LBL-6545, June, (1977).

16. J. Bond, P. J. Johansen, S. E. Koonin, and S. Garpman, Phys. Lett. 71B, 43 (1977).

17. J. I. Kapusta, Phys. Rev. C 16, 1493 (1977).

18. See Ref. 1 and references therein.

19. In principle there could be effects which depend on the length of the streaks, for instance if one does not assume completely inelastic collisions between streaks.

20. E. Segrè, Nuclei and Particles (Benjamin, New York, 1964), p. 635.

21. S. Fiarman and S. S. Hanna, Nucl. Phys. A251, 1 (1975).

22. S. Fiarman and W. E. Meyerhof, Nucl. Phys. A206, 1 (1973).

23. F. Ajzenberg-Selove and T. Lauritsen, Nucl. Phys. A227, 1 (1974).

24. The computer code written to perform the calculations described in this section is available.

25. This is in contrast to the coalescence model which requires a separate parameter for each nuclear fragment. This parameter also varies somewhat with beam energy. See Ref. 1 and references therein.

26. See Ref. 1. We thank the authors for allowing us the use of some of their unpublished data.

27. In this regard see M. Gyulassy and S.K. Kauffmann, Phys. Rev. Lett. 40, 298 (1978).

FIGURE CAPTIONS

Fig. 1 Spectra of protons in the lab from the bombardment of U by Ne at 400 and 2100 MeV/nucleon. Data is from Ref. 1. See text concerning the 2100 MeV/nucleon data. The model predictions have been multiplied by 2.

Fig. 2 Spectra of deuterons in the lab from the bombardment of U by Ne at 400 and 2100 MeV/nucleon. Data is from Ref. 1. See text concerning the 2100 MeV/nucleon data. The model predictions have been multiplied by 2.

Fig. 3 Spectra of tritons in the lab from the bombardment of U by Ne at 400 and 2100 MeV/nucleon. Data is from Ref. 1. See text concerning the 2100 MeV/nucleon data. The model predictions have been multiplied by 2.

Fig. 4 Spectra of ^{3}He in the lab from the bombardment of U by Ne at 400 and 2100 MeV/nucleon. The model predictions have been multiplied by 2. Data is from Ref. 1.

Fig. 5 Spectra of ^{4}He in the lab from the bombardment of U by Ne at 400 and 2100 MeV/nucleon. Data is from Ref. 1. The model predictions have been multiplied by a factor of 4 and 6 respectively.

Fig. 6 Invariant cross section vs. lab momentum for protons from the bombardment of Cu and Be by Ar at 1800 MeV/nucleon. Data is from Ref. 2.

Fig. 7 Invariant cross section vs. lab momentum for deuterons from the bombardment of Cu and Be by Ar at 1800 MeV/nucleon. Data is from Ref. 2.

Fig. 8 Invariant cross section vs. lab momentum for tritons from the bombardment of Cu and Be by Ar at 1800 MeV/nucleon. Data is from Ref. 2.

Fig. 9 Invariant cross section vs. rapidity at fixed transverse momentum for protons from the bombardment of Pb by Ne at 800 MeV/nucleon. The dashed line represents the nucleon-nucleon center of mass frame. Error bars (not shown) range from 20% for the large cross sections to 100% for the small cross sections. Data is from Ref. 3.

Fig. 10 Invariant cross section vs. rapidity at fixed transverse momentum for negative pions from the bombardment of Pb by Ne at 800 MeV/nucleon. The dashed line represents the nucleon-nucleon center of mass frame. Error bars (not shown) range from 20% for the large cross sections to 100% for the small cross sections. Data is from Ref. 3.

Fig. 11 Invariant cross section vs. rapidity at fixed transverse momentum for protons from the bombardment of NaF by Ne at 800 MeV/nucleon. Error bars (not shown) range from 20% for the large cross sections to 100% for the small cross sections. Data is from Ref. 3.

Fig. 12 Invariant cross section vs. rapidity at fixed transverse momentum for negative pions from the bombardment of NaF by Ne at 800 MeV/nucleon. Error bars (not shown) range from 20% for the large cross sections to 100% for the small cross sections. Data is from Ref. 3.

Fig. 13 Spectrum of positive pions in the lab from the bombardment of Pb by Ne at 800 MeV/nucleon. Data is from Ref. 4. The model predictions have been multiplied by 1/2.

Fig. 14 Spectrum of positive pions in the lab from the bombardment of NaF by Ne at 800 MeV/nucleon. Data is from Ref. 4. The model predictions have been multiplied by 1/2.

Fig. 15 Temperature vs. η for three bombarding energies.

Fig. 16 Ratio of the number of nucleons to the baryon number in the final state vs. η.

Fig. 17 Ratio of the number of pions to the baryon number in the final state vs. η.

TABLE I. Grouping of nuclear resonances into effective resonances used in the calculations.

nucleus	Excitation Energy above g.s.	J^P	decay modes	effective decay mode	$\frac{\Sigma(2S_i+1)E_i}{\Sigma(2S_i+1)}$ ↓ effective Ex. Energy	$\Sigma(2S_i+1)$ ↓ effective (2S+1)
^2H	2.2	1^+	p+n	p+n	2.2	boson 3
^4H	0(-5.1)[a]	2^-	^3H+n			boson
	1.7	1^-	"	^3H+n	1.6	11
	4.1	1^-	"			
^4He	20.1	0^+	p			
	21.1	0^-	p,n	1/2(^{3}He+n)		boson
	22.1	2^-	p,n	+		
	25.5	0^+	---	1/2(^{3}H+p)	27.5	
	26.4	2^-	p,n			28
	27.4	1^-	p,n,γ			
	29.5	0^-	p,n			
	30.5	1^-	p,n,γ			
	31.0	1^-	p,n,d			
	33.0	2^+	p,n,d			
^4Li	0(-3.0)[a]	2^-	^{3}He+p			boson
	1.4	1^-	"	^{3}He+p	1.9	12
	3.2	0^-	"			
	5.0	1^-	"			
^5He	0(0.9)[a]	$3/2^-$	n,α			fermion
	4.0	$1/2^-$	n,α	^{4}He+n	11.1	14
	16.8	$3/2^+$	γ,n,d,t,α			
	19.9	$3/2^+$	n,d,t,α			
^5Li	0(1.9)[a]	$3/2^-$	p,α			fermion
	4.0	$1/2^-$	p,α	^{4}He+p	11.9	16
	16.7	$3/2^+$	γ,p,d,^{3}He,α			
	18.0	$1/2^+$	γ,p,d,^{3}He,α			
	20.0	$3/2^+$	γ,p,d,^{3}He,α			

[a]The numbers in parentheses refer to the binding energy with respect to the constituent nucleons.

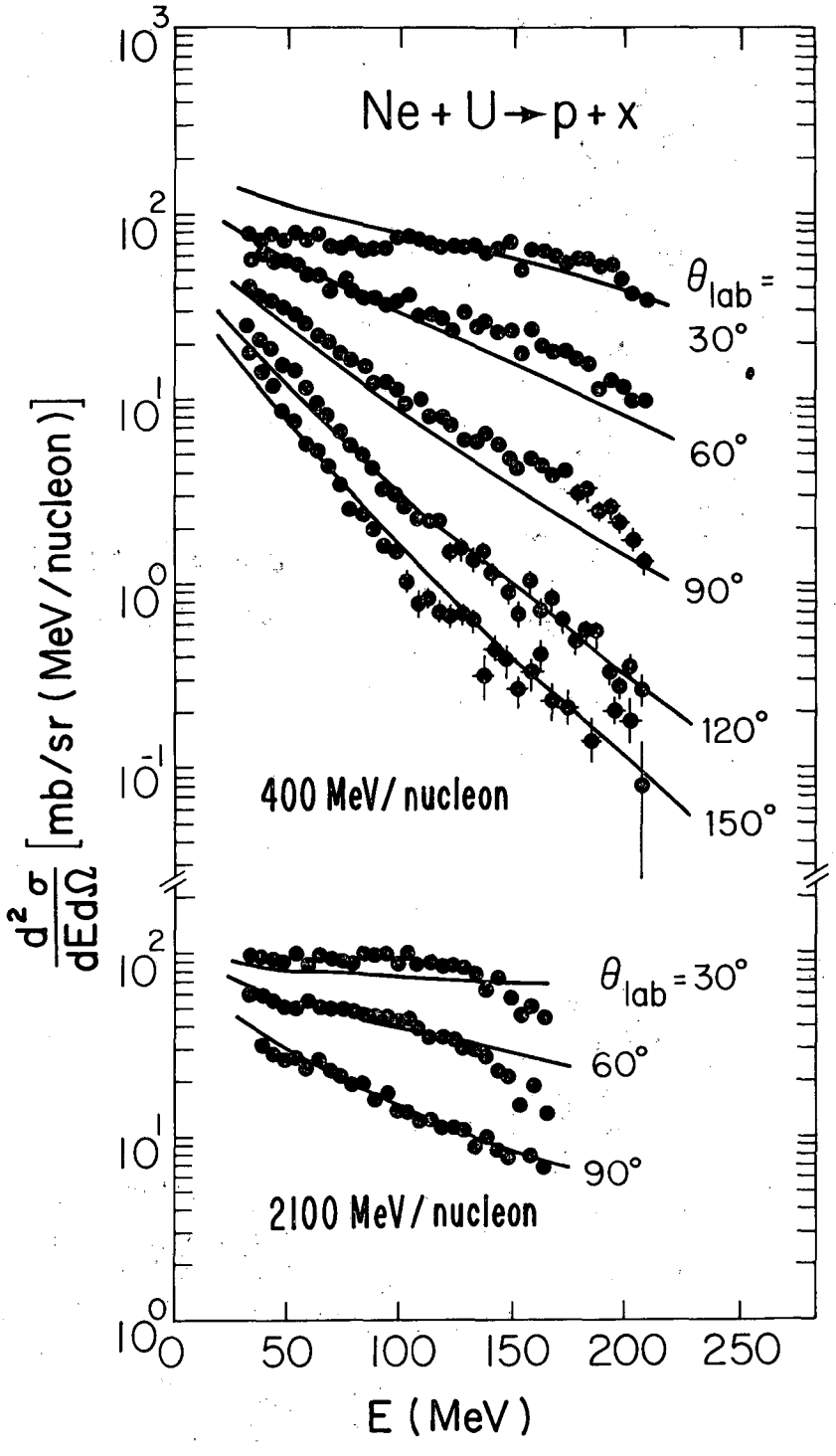
Ne + U → p + x
θ_{lab} =
30°
60°
90°
120°
150°
400 MeV/ nucleon
θ_{lab} = 30°
60°
90°
2100 MeV/ nucleon
$\frac{d^2\sigma}{dEd\Omega}$ [mb/sr (MeV/nucleon)]
E (MeV)
XBL7711-11413

FIG. 1

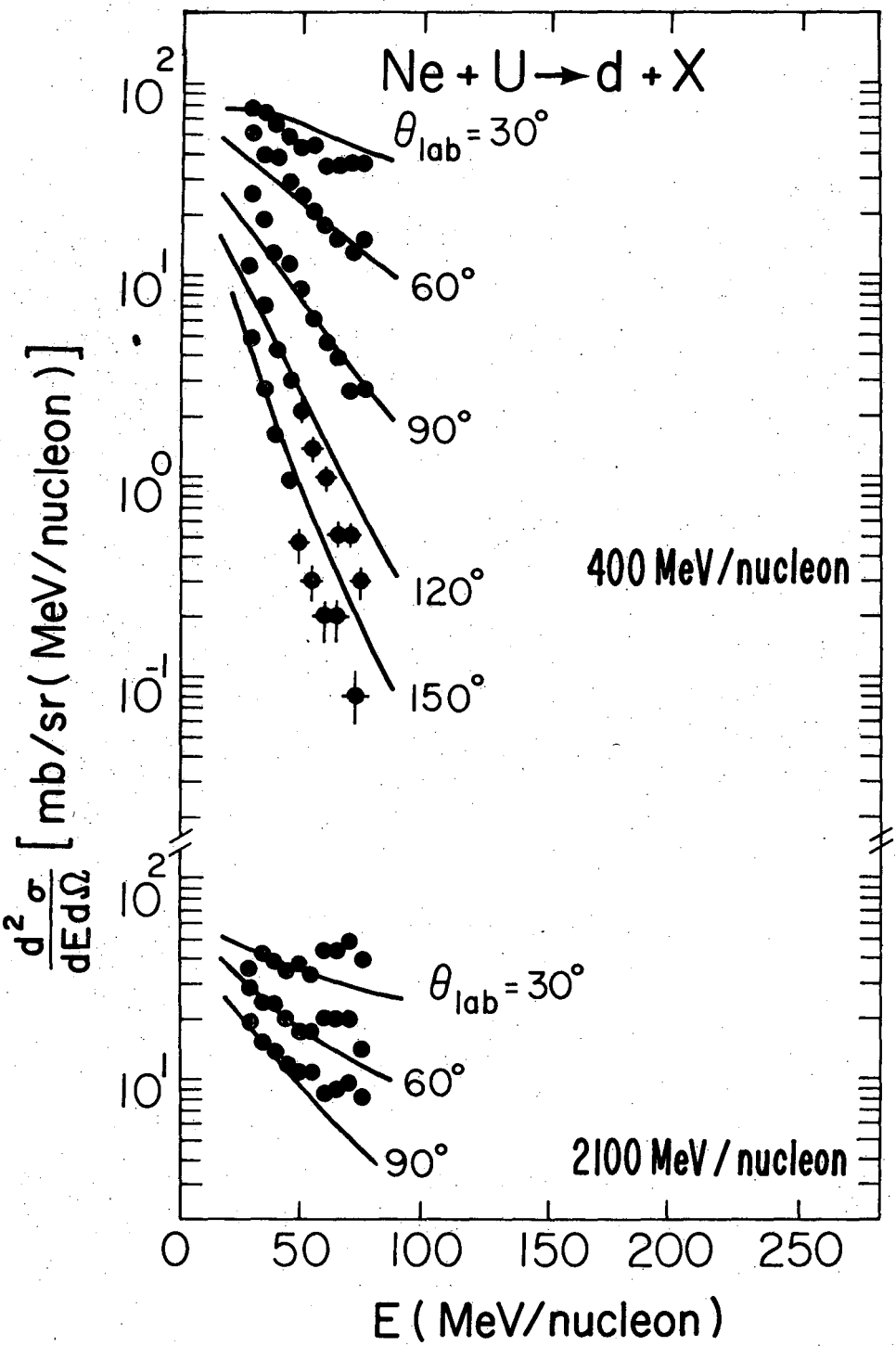

FIG. 2

XBL 78-65

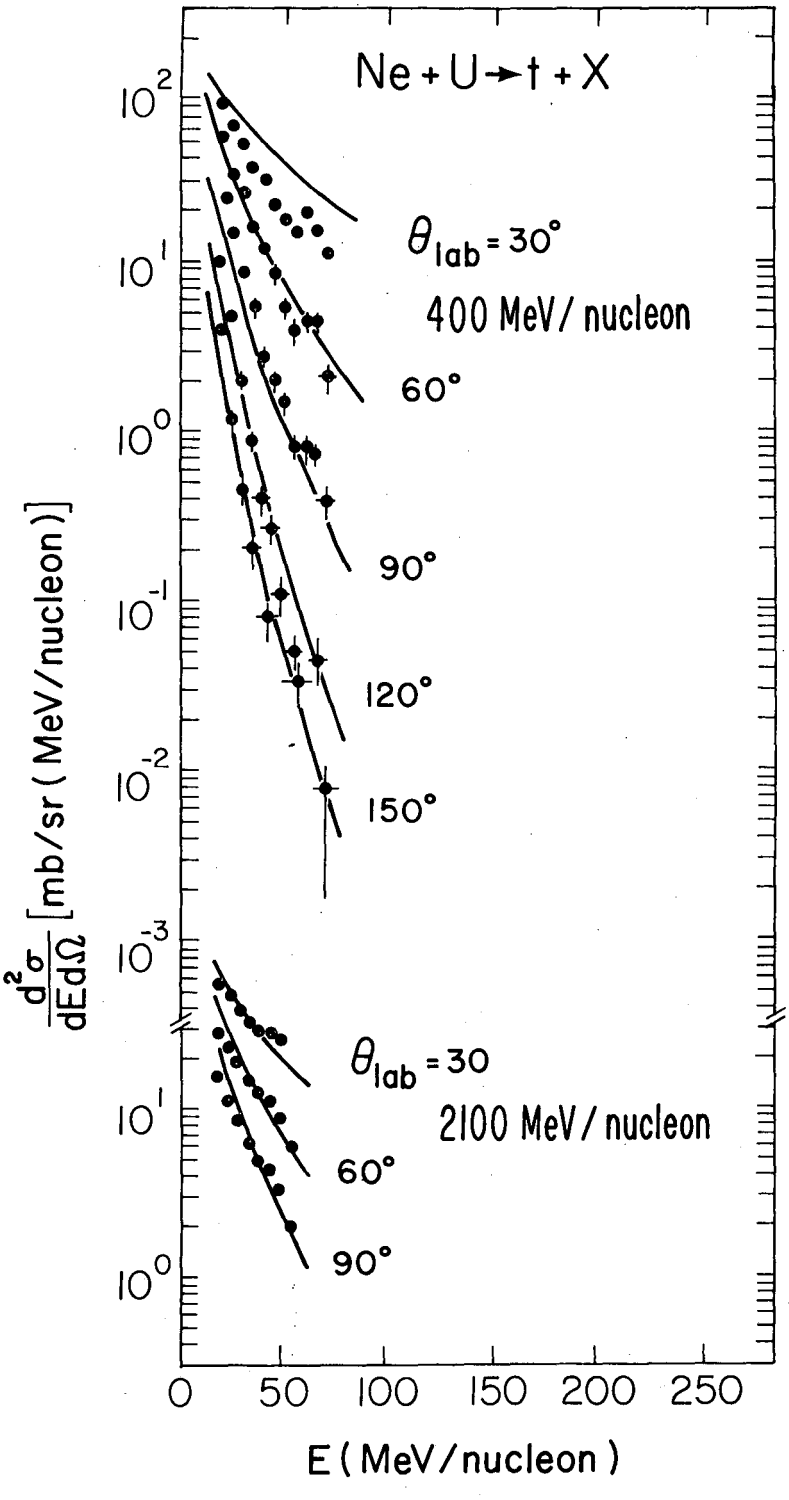

FIG. 3

XBL7711-11411

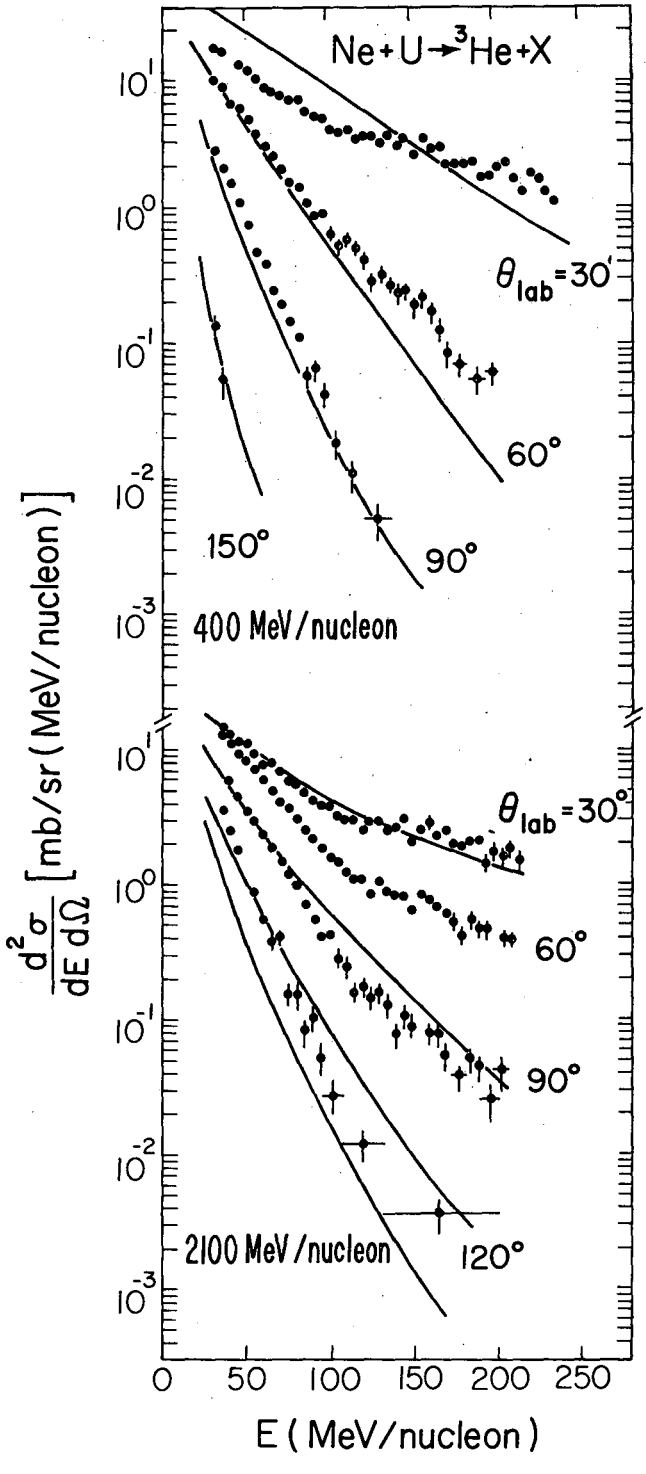

FIG. 4

XBL 781-64

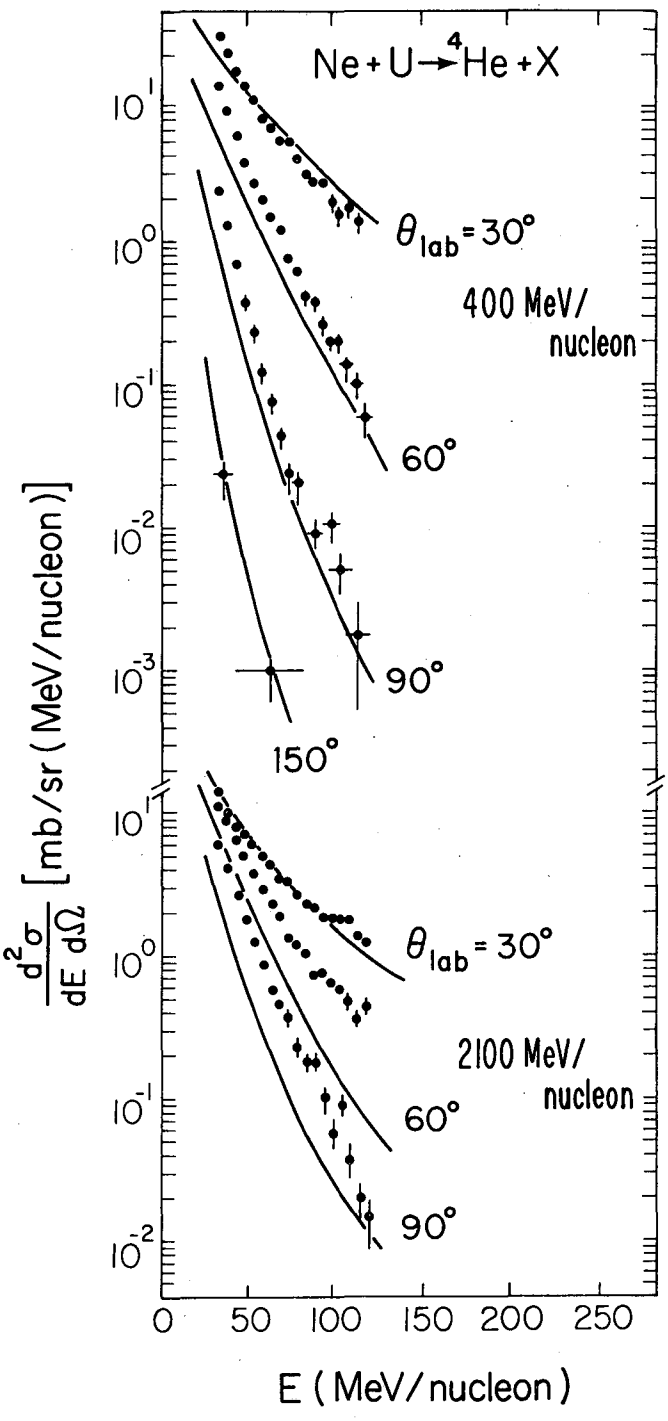

FIG. 5

XBL 781-63

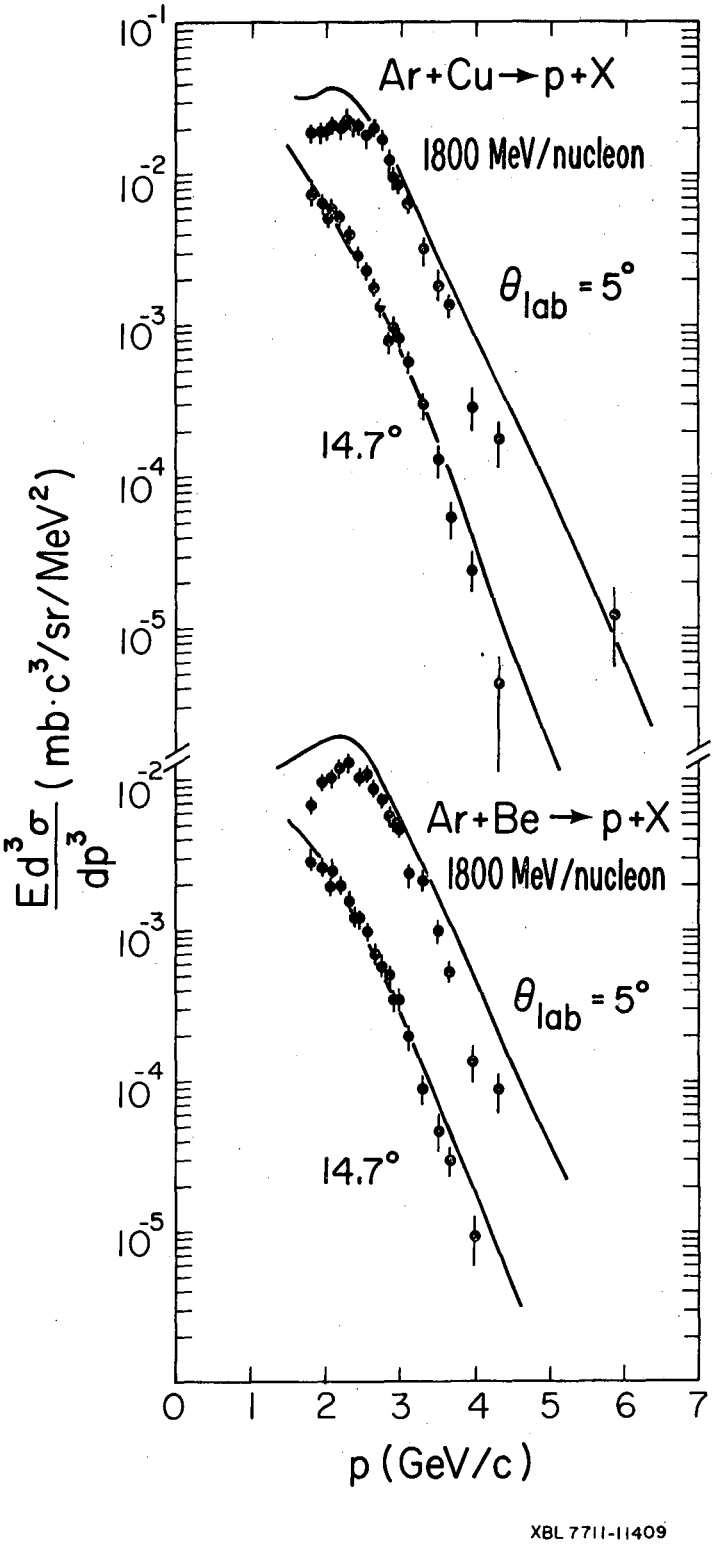
Ar+Cu→p+X
1800 MeV/nucleon
θlab = 5°
14.7°
Ar+Be→p+X
1800 MeV/nucleon
θlab = 5°
14.7°
Ed³σ/dp³ (mb·c³/sr/MeV²)
p (GeV/c)
XBL 7711-11409

FIG. 6

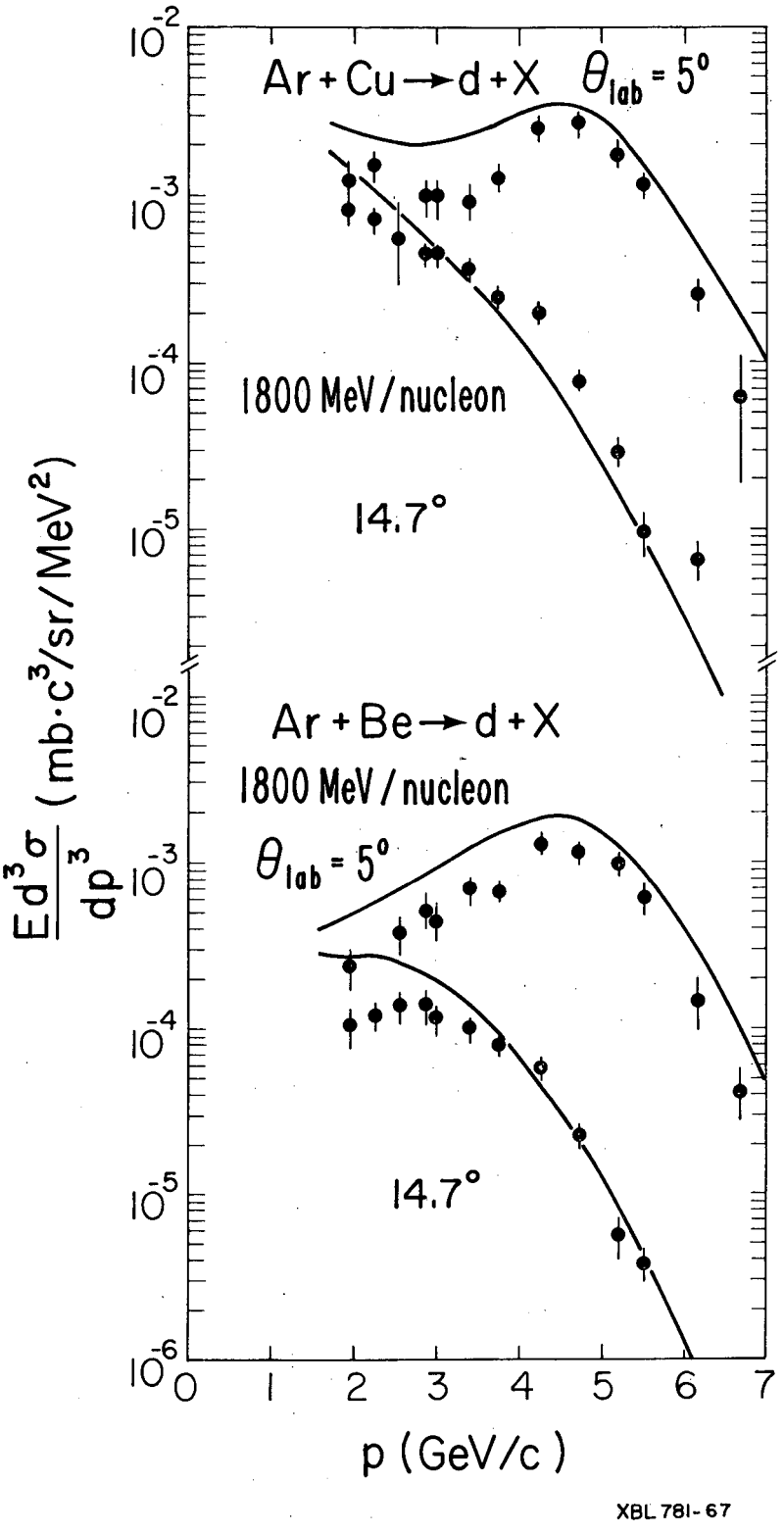
Ar + Cu → d + X θlab = 5°
1800 MeV/nucleon
14.7°
Ar + Be → d + X
1800 MeV/nucleon
θlab = 5°
14.7°
Ed³σ/dp³ (mb·c³/sr/MeV²)
p (GeV/c)
XBL 781-67

FIG. 7

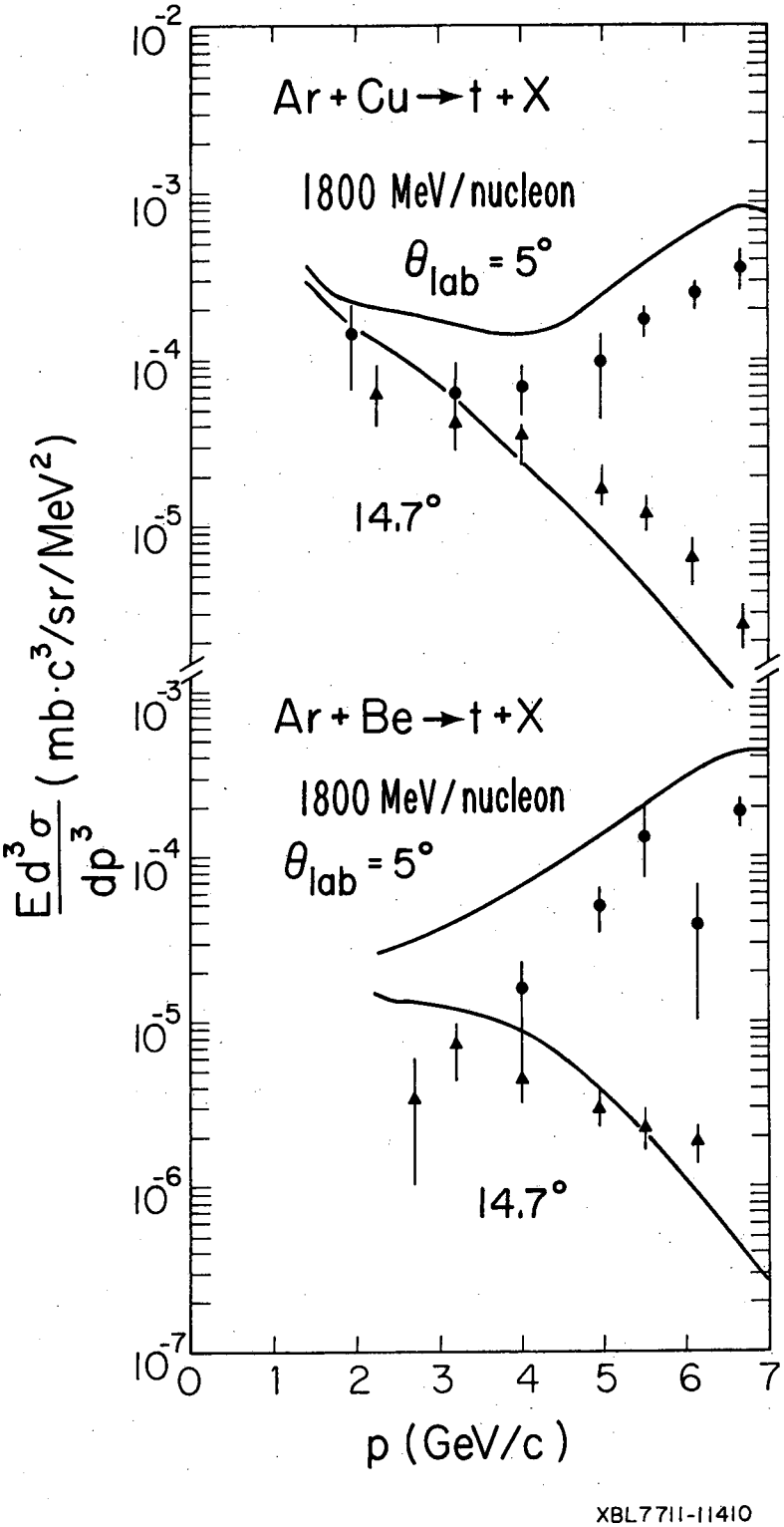
Ar + Cu → t + X
1800 MeV/nucleon
θlab = 5°
14.7°
Ar + Be → t + X
1800 MeV/nucleon
θlab = 5°
14.7°
Ed³σ/dp³ (mb·c³/sr/MeV²)
p (GeV/c)
XBL7711-11410

FIG. 8

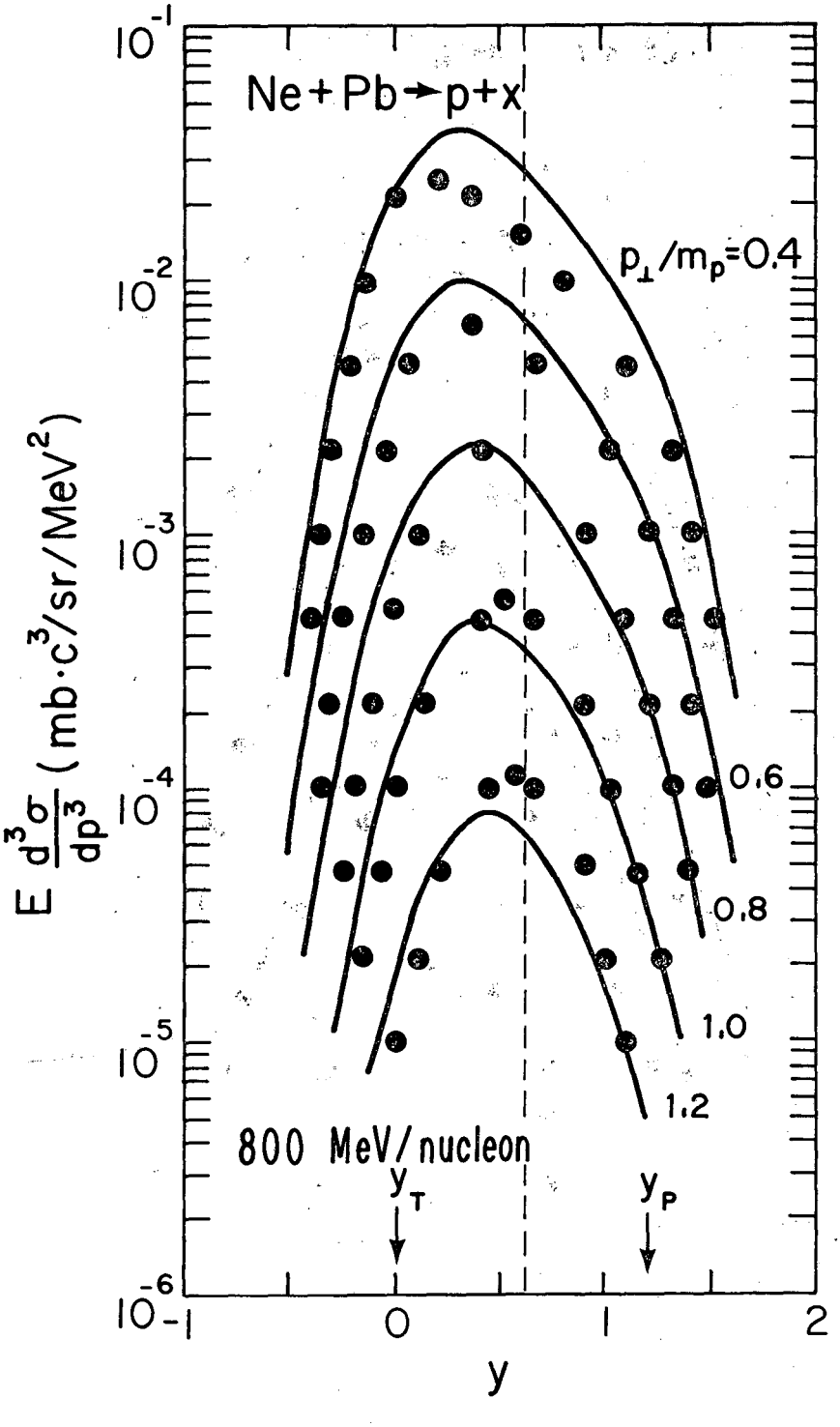

XBL 7711-11412

FIG. 9

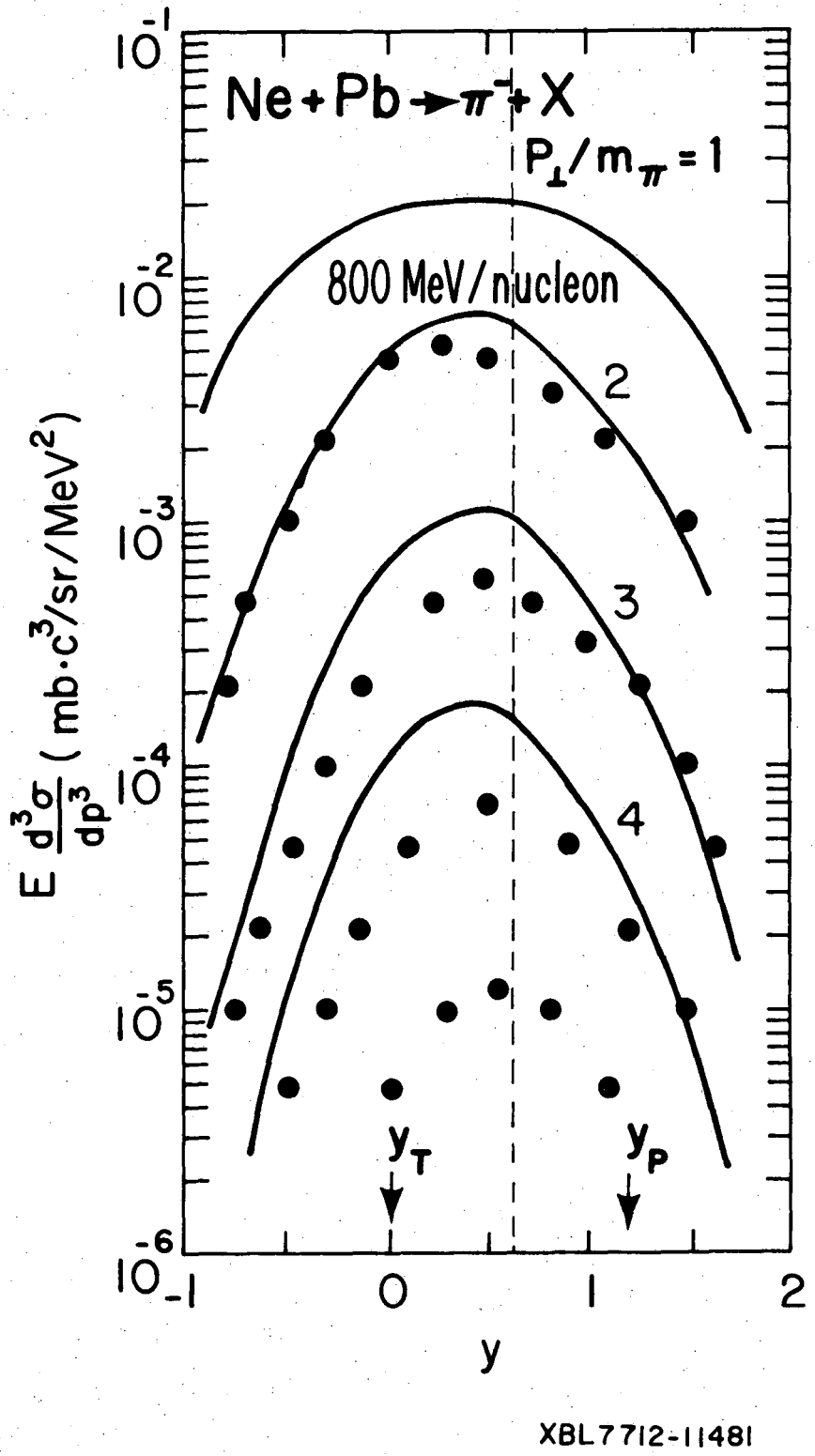

XBL7712-11481

FIG. 10

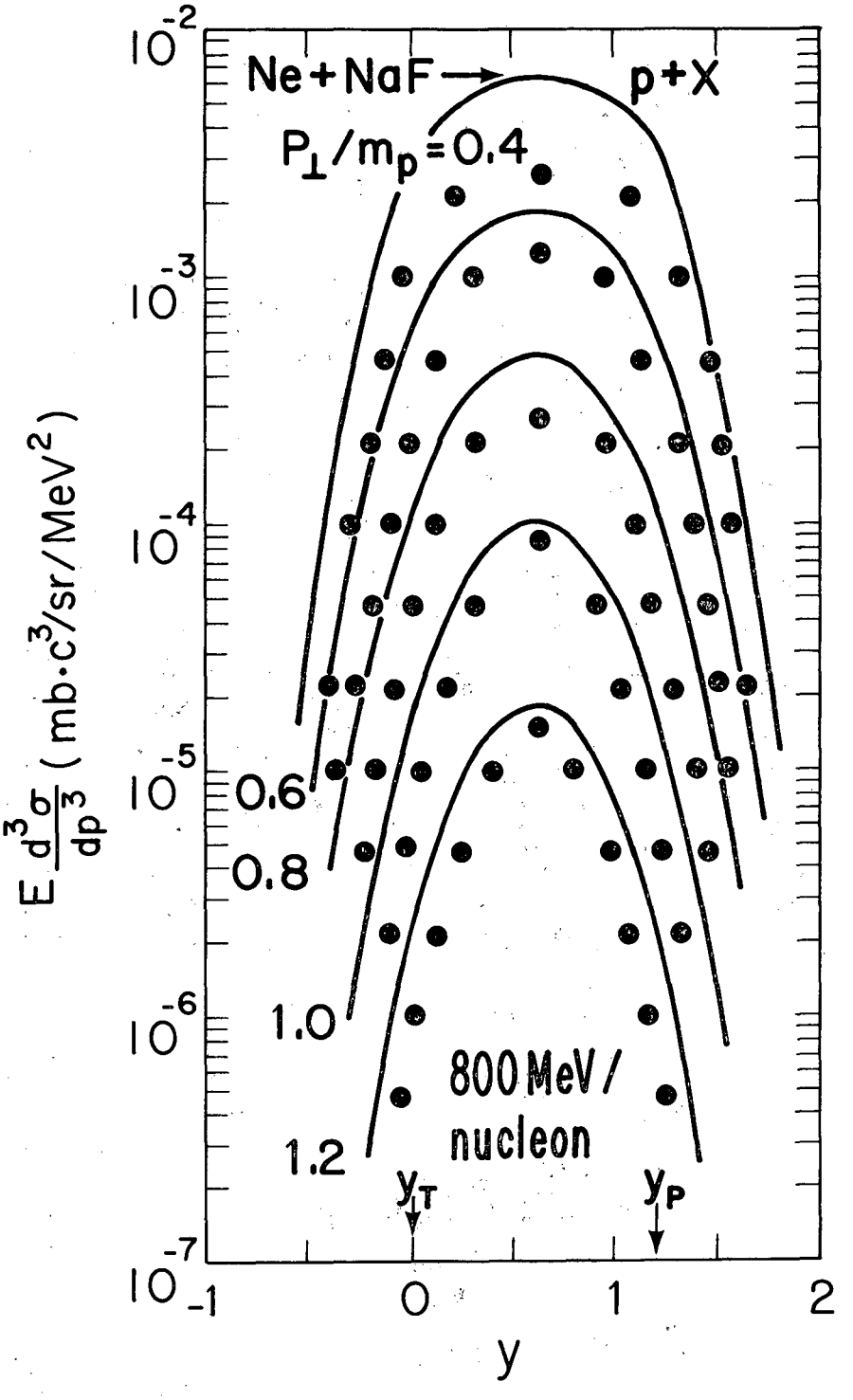

XBL 781-66

FIG. 11

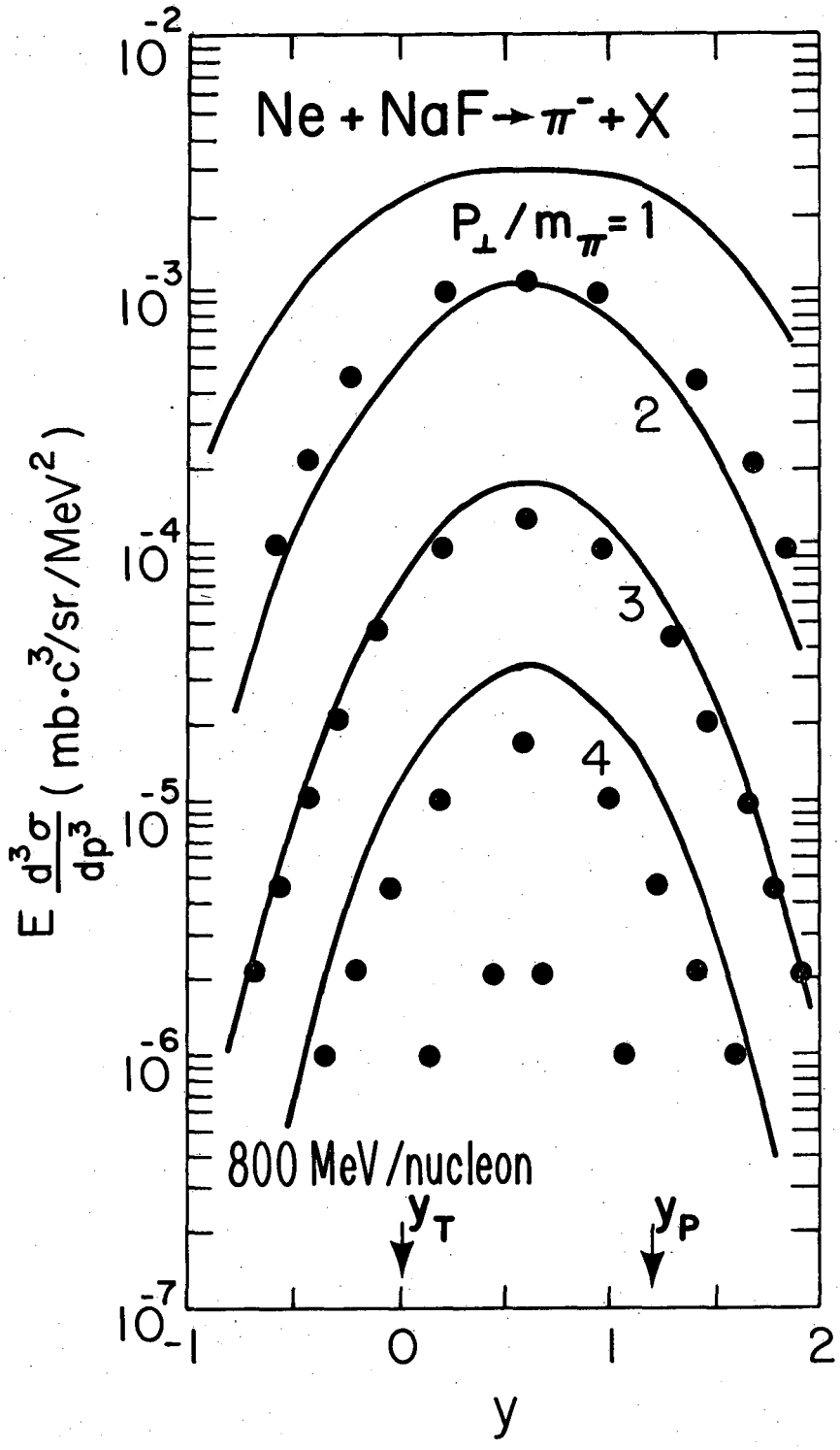

XBL781-59

FIG. 12

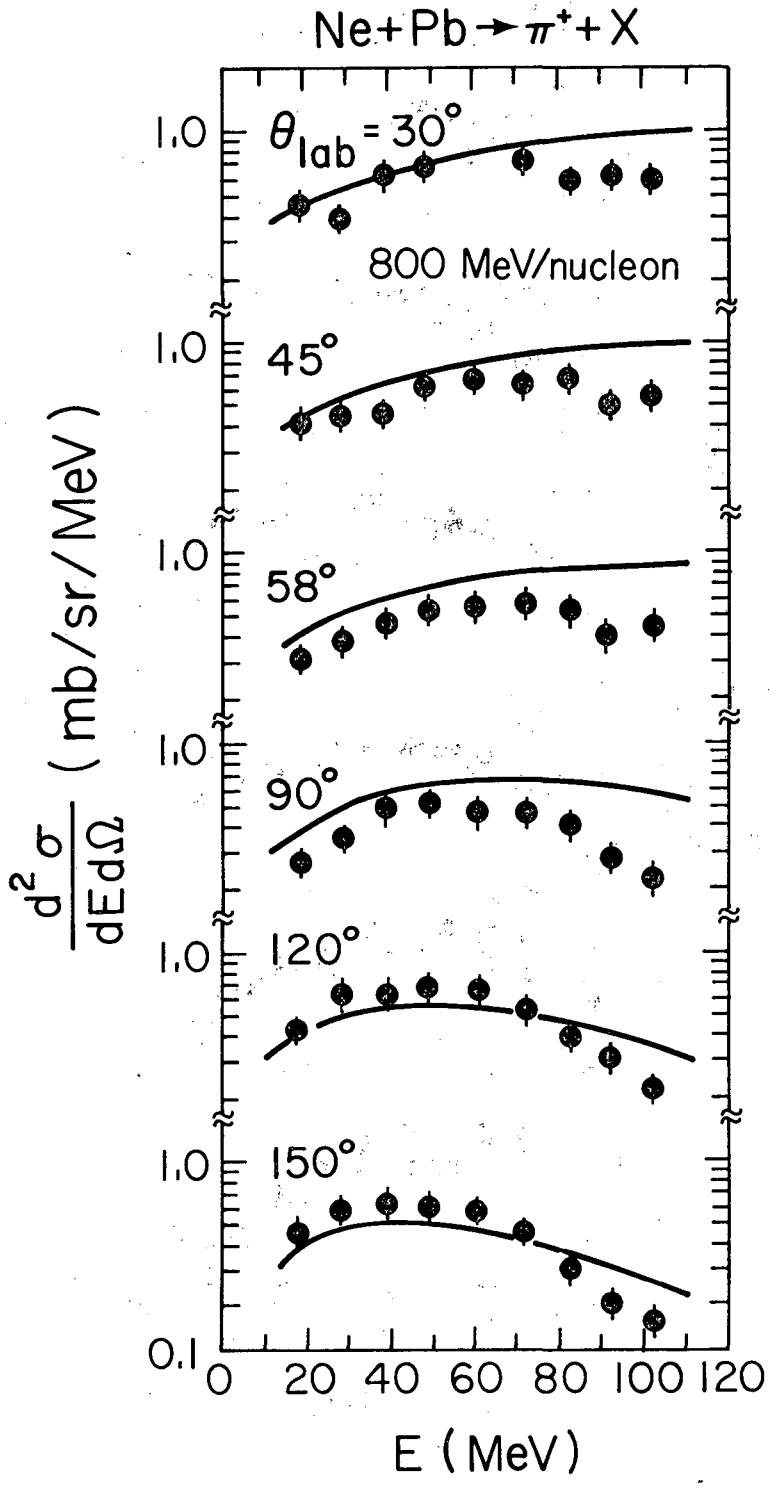

XBL7711-11414

FIG. 13

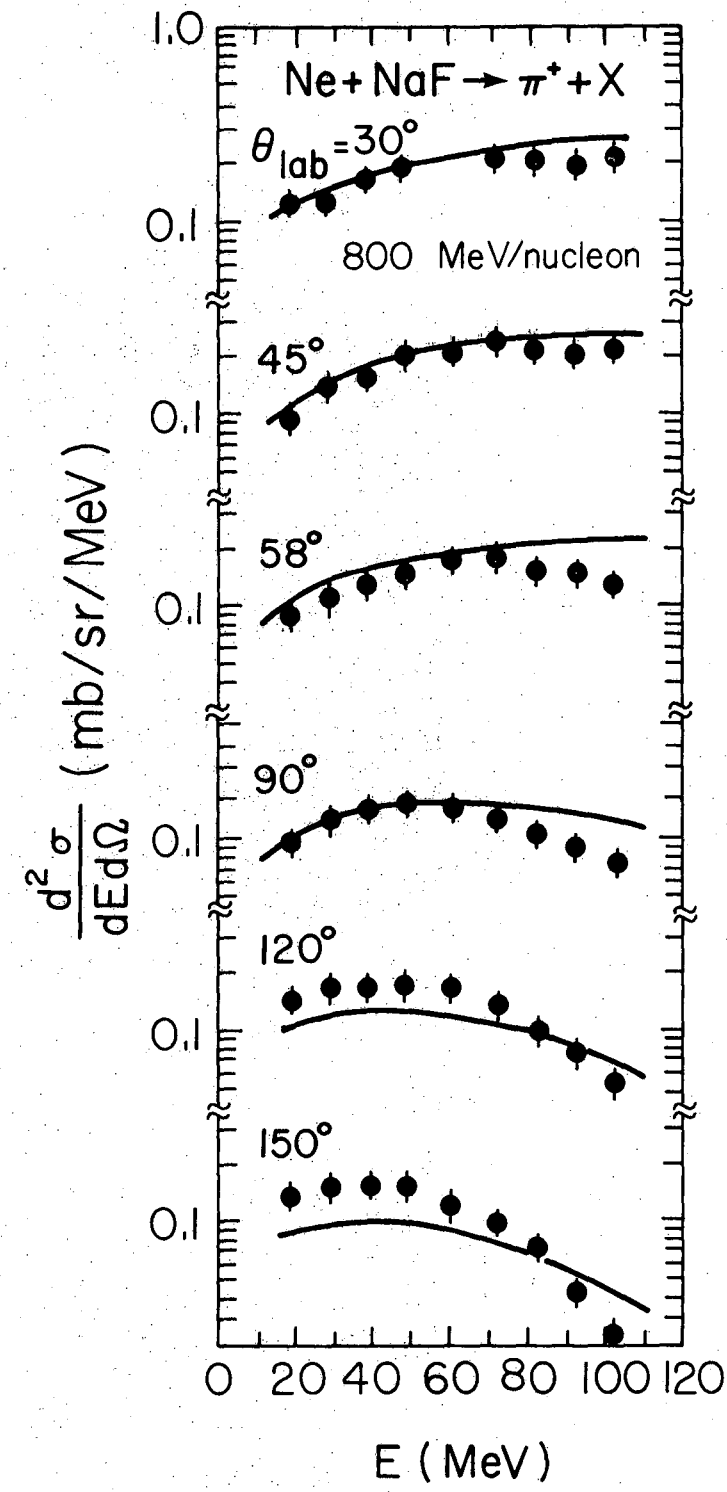
Ne+NaF → π⁺+X
θlab=30°
800 MeV/nucleon
45°
58°
90°
120°
150°
1.0
0.1
0 20 40 60 80 100 120
E (MeV)
d²σ/dEdΩ (mb/sr/MeV)
XBL7711-11415

FIG. 14

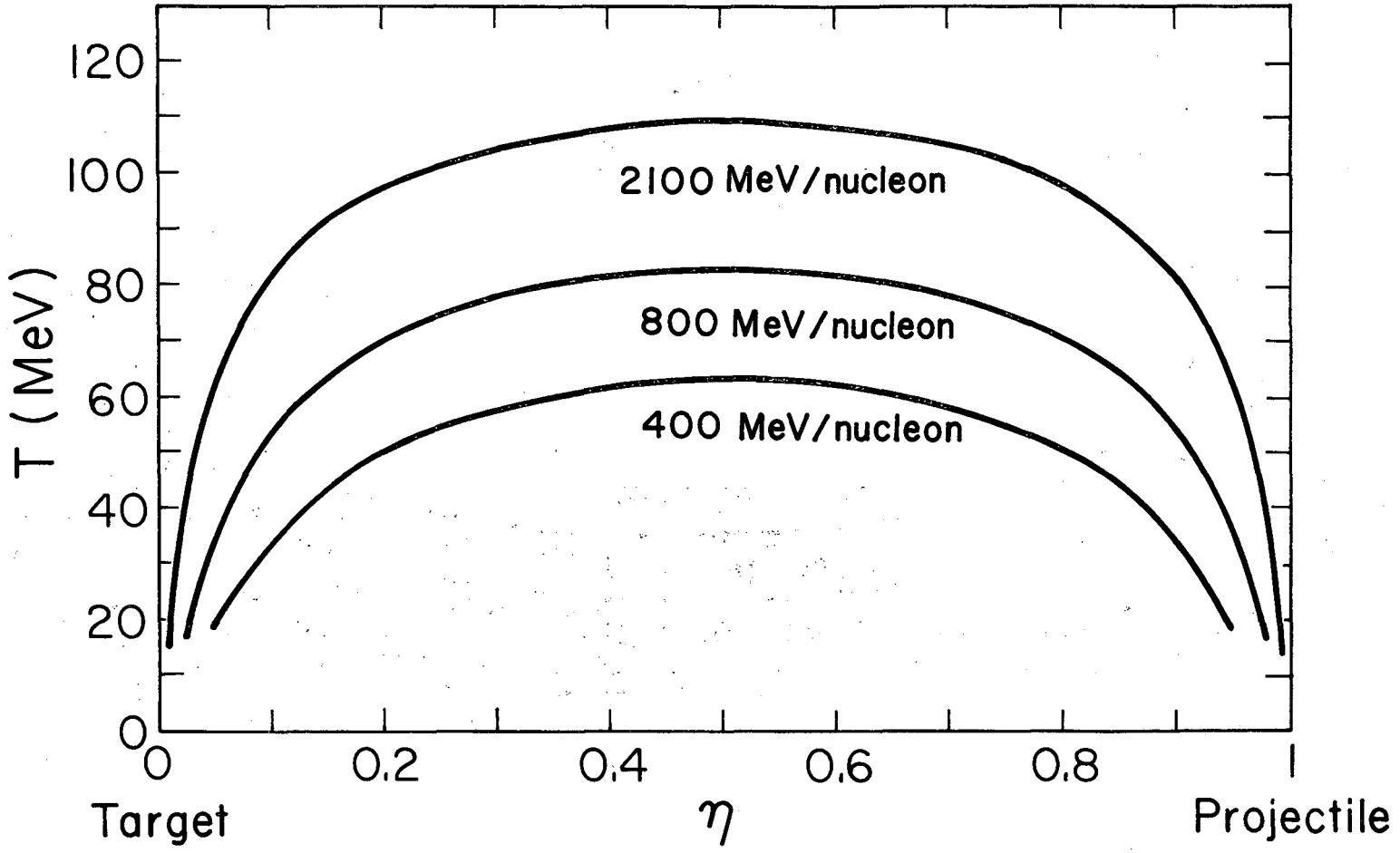

XBL 781-62

FIG. 15

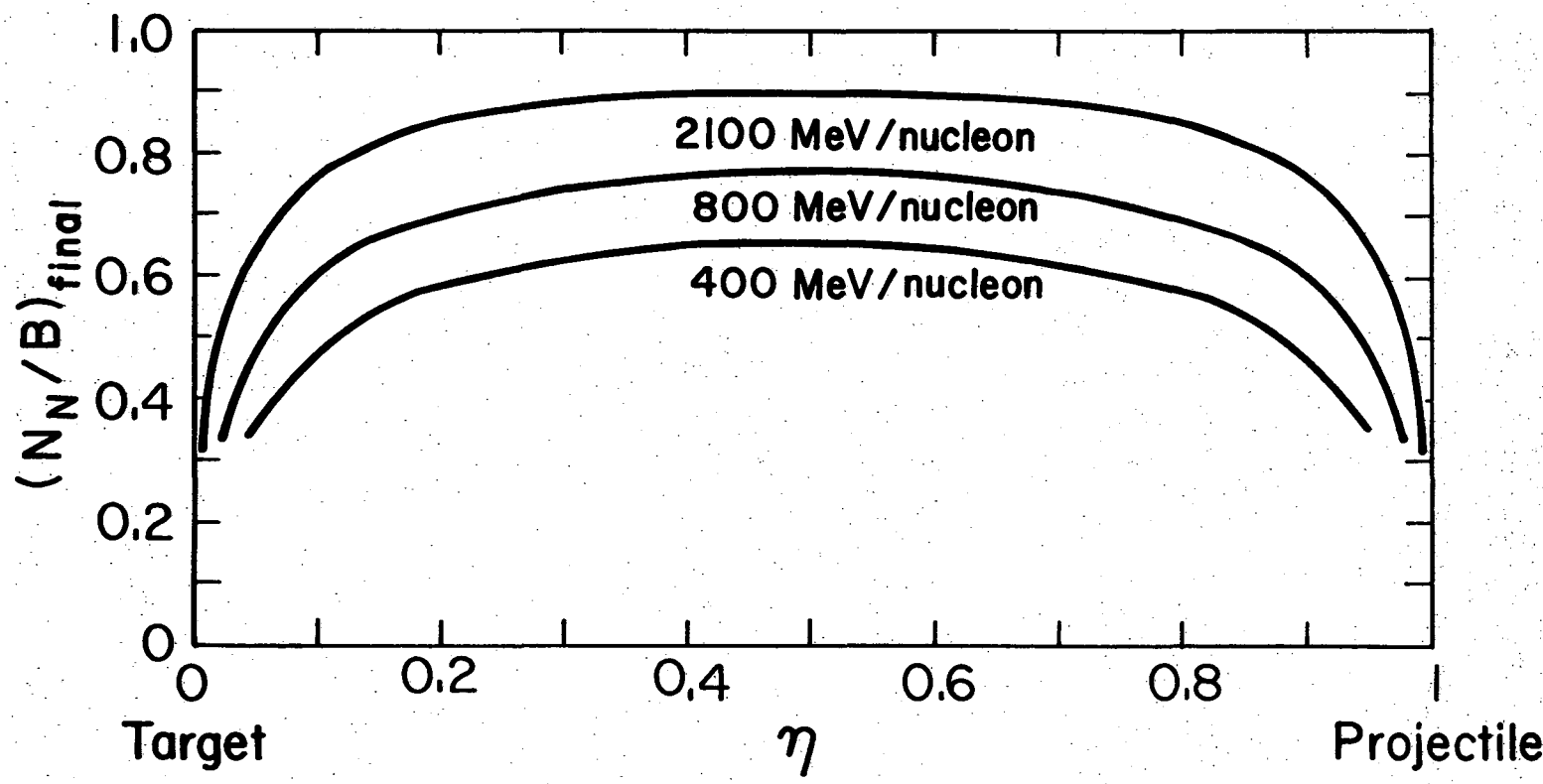

XBL 781-60

FIG. 16

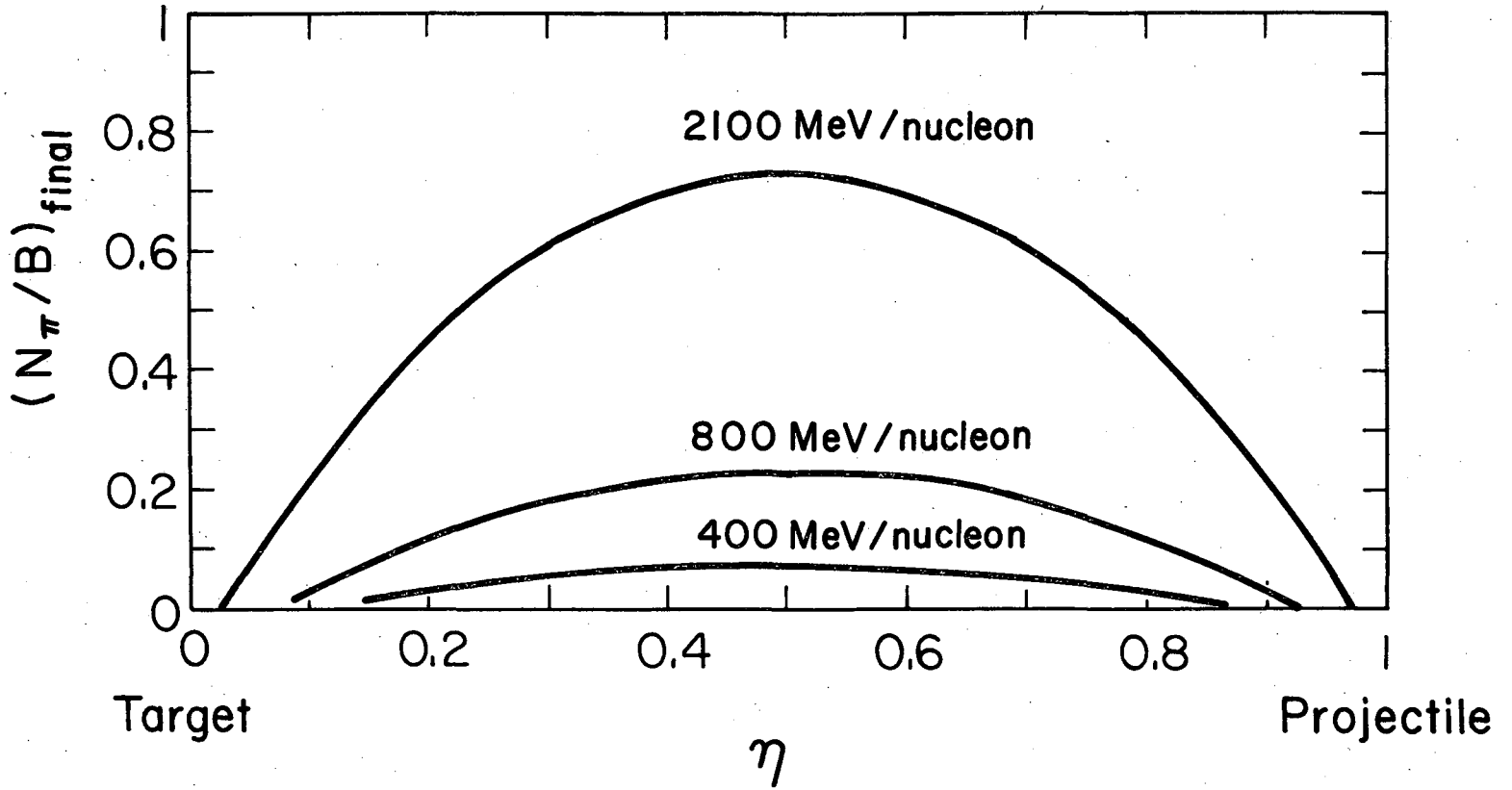

XBL 781-61

FIG. 17

This report was done with support from the Department of Energy. Any conclusions or opinions expressed in this report represent solely those of the author(s) and not necessarily those of The Regents of the University of California, the Lawrence Berkeley Laboratory or the Department of Energy.

TECHNICAL INFORMATION DEPARTMENT
LAWRENCE BERKELEY LABORATORY
UNIVERSITY OF CALIFORNIA
BERKELEY, CALIFORNIA 94720